Scientific Insights from Four Generations of Lagrangian Smart Balloons in Atmospheric Research*

BY S. BUSINGER, R. JOHNSON, AND R. TALBOT

NOAA's autonomous balloons, capable of crossing oceans and sampling at very low altitudes, use advanced instrument and communication technology to create new research opportunities.

Small instrumented balloons designed and constructed at the National Oceanic and Atmospheric Administration (NOAA) Air Resources Laboratory Field Research Division (ARLFRD) were released during a series of recent field experiments[1] to provide in situ data and airmass tracking information (Fig. 1, appendix). The field experiments were largely a part of the International Global Atmospheric Chemistry (IGAC) program designed to study the chemical, physical, and radiative properties and processes of atmospheric pollution and aerosols. A better understanding of these complex interactions is needed to construct accurate numerical models of local pollution episodes, as well as models of future global climate. Evolution of the marine boundary layer and air–sea exchange has also been a focus of

[1] The Atlantic Stratocumulus Transition Experiment/Marine Aerosol Gas Exchange (ASTEX/MAGE) field project, the first and second Aerosol Characterization Experiments (ACE-1, ACE-2), the International Consortium for Atmospheric Research on Transport and Transformation (ICARTT), Rainband and Intensity Change Experiment (RAINEX), and planned deployment in the second Texas Air Quality Study (TexAQS II).

*School of Ocean and Earth Science and Technology Contribution Number 6790

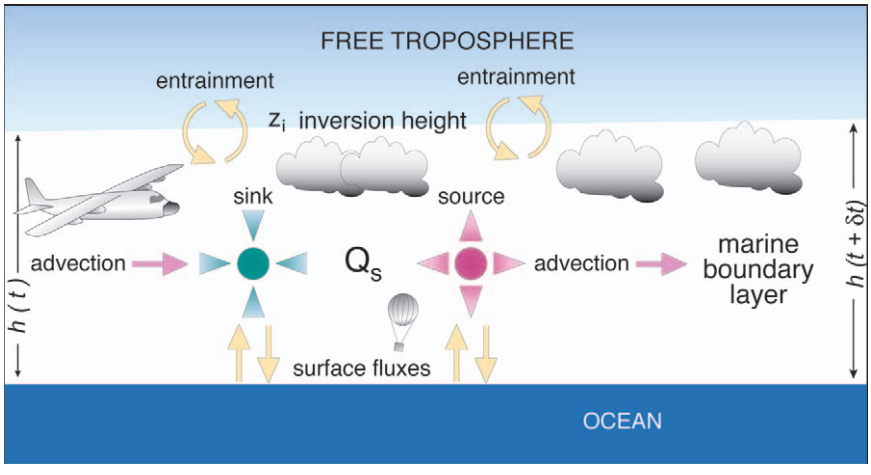

FIG. 1. Schematic illustration of the terms in the mean concentration budget for a scalar variable in the marine boundary layer with a net internal source or sink Q_s (adapted from Johnson et al. 2000).

these field experiments. The availability of affordable, lightweight GPS receivers and satellite cellular communication enables us to receive low-altitude in situ data in an air mass that can be tracked anywhere in the world.

A frame of reference that moves with the air is a natural choice for pollution and aerosol studies (Seinfeld et al. 1973; Angell et al. 1973; Suhre et al. 1998). This reference frame is commonly called *Lagrangian* after the inventor, French mathematician Joseph Louis Lagrange (1736–1813). In total, 10 Lagrangian experiments were carried out—2 each during the ASTEX/MAGE and ACE-1 field programs, and 3 each during the ACE-2 and ICARTT field programs. This paper traces the innovations in design and gains in capability of the autonomous Lagrangian balloons. Progress in our understanding of the relationships between the evolution of marine boundary layers and the atmospheric chemistry contained therein as a result of the application of the NOAA balloons in Lagrangian experiments is reviewed to provide a context for the significance of the balloon development program to our science.

In Lagrangian experiments the focus is on a volume of air of limited extent as that volume is transported with the wind (Fig. 1). A Lagrangian strategy offers distinct benefits over studies in which measurements are made only at fixed sites. Researchers can concentrate measurement resources, such as a research aircraft, in a moving air volume. Consequently, with a fixed level of available resources, more data can be obtained on the behavior of the species of interest in this volume than would be obtained if the same resources were uniformly deployed over the entire region of potential interest—an important consideration for long-range studies (Angell 1974). Businger et al. (1996) provide a comprehensive review of the application of balloons as markers in a Lagrangian strategy. For earlier balloon applications see also Harrison (1957), Angell (1975), and Zak (1981).

Lateral flow into and out of a Lagrangian volume is typically much less than that for a comparable volume because the mean wind in the Lagrangian frame of reference is approximately zero (Fig. 1). A first-order approximation sometimes employed is to assume that the volume is isolated from its surroundings and to treat exchange as a perturbation. A Lagrangian experiment can best remove tendencies in fields due to horizontal advection under one of the following conditions: i) there is no mean vertical wind shear within the boundary layer, or ii) there is mean vertical shear, but rapid turbulent vertical circulations keep all air parcels eddying along at the same mean rate. In this latter case, the mass-weighted average horizontal velocity should be used to advect the column of boundary layer air. It should be noted, however, that shear does manifest as transport through the walls of Fig. 1, and can result in the dispersion of airmass properties. Having good control of the altitude of the balloon is critical to a successful experiment under conditions of wind shear in order for the balloon trajectory to reflect the mass-weighted average velocity of the layer being sampled. The impact of wind shear on the results of a Lagrangian strategy depends on the magnitude and nature (direction versus speed) of the shear and also on the distribution of sources and sinks for the species being measured. For example, when plumes of pollution originating from point sources are being tracked, significant directional shear of the horizontal wind can cause difficulties in the interpretation of balloon-based observations. The success of other applications of the Lagrangian strategy, such as estimates of surface fluxes into a marine boundary layer, are in general less sensitive to wind shear. Consequently, in timing the start of Lagrangian experiments, care must be given in choosing the synoptic conditions and the best altitude for the balloon measurements to optimize the success of the Lagrangian strategy given the aims of the experiment. A quantitative analysis of the impact of shear on the Lagrangian strategy is case dependent and will continue to be an area of active research (e.g., Siems et al. 2000).

Time evolution is the fundamental strength of Lagrangian measurements, which can corroborate output from Lagrangian numerical models (Hoecker 1981; Suhre et al. 1998). Although Lagrangian models themselves may not be optimal for regulatory purposes, they are invaluable investigative tools for developing an understanding of the processes fundamental to the chemistry and physics of air pollution

AFFILIATIONS: Businger—Department of Meteorology, University of Hawaii, Honolulu, Hawaii; Johnson—NOAA, ARLFRD, Idaho Falls, Idaho; Talbot—University of New Hampshire, Durham, New Hampshire
CORRESPONDING AUTHOR: S. Businger, University of Hawaii, Department of Meteorology, 2525 Correa Rd., Honolulu, HI 96822
E-mail: businger@hawaii.edu

The abstract for this article can be found in this issue, following the table of contents.
DOI:10.1175/BAMS-87-11-1539

In final form 8 June 2006

and the dynamics of storms, an understanding that can only be tested with Lagrangian experiments.

It has been a goal of the NOAA Lagrangian balloon development program to continually improve the capability and performance of the smart balloons. Significant advances have been made in our ability to communicate with the smart balloons, to accurately ascertain their position, and to control their altitude. GPS data from five equally ballasted tetroons that are released together can be used to derive the full kinematics (divergence, vorticity, and shear and stretching deformation) of the air in which they reside. Naturally, cost and logistics have become important considerations in subsequent field experiments as the complexity and capabilities of individual balloons increase, limiting multiple balloon releases to two or three balloons during more recent field experiments.

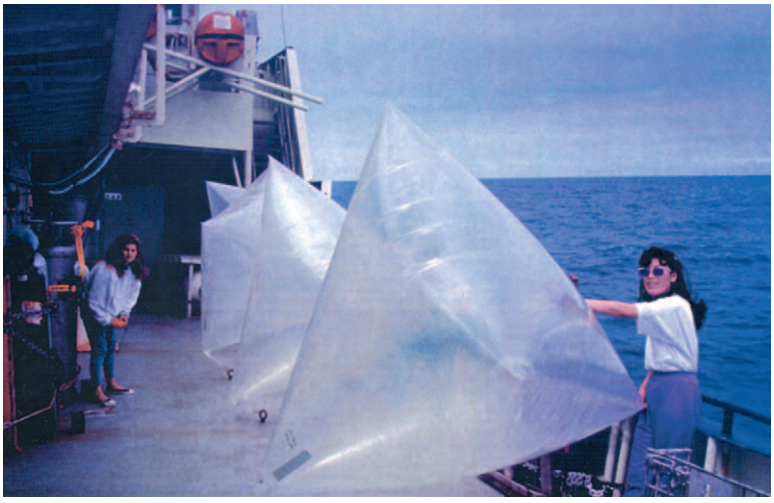

Fig. 2. Shipboard deployment of Lagrangian marker tetroons during ASTEX/MAGE, June 1992 (adapted from Businger et al. 1996).

A fundamental constraint for unmanned balloon systems deployed in U.S. air space is the limitation set forth by the Federal Aviation Administration[2] that the combined weight of the transponder, batteries, and instruments must be less than 12 lb (5.4 kg), with no one package weighing more than 6 lb. Above this weight limit, balloons must carry expensive and heavy warning beacons, and they are subject to additional restrictions, providing strong motive to miniaturize the instrument packages.

Energy consumption by the instruments and transponder is a critical factor that is closely related to the weight restriction, by virtue of the high-energy density of batteries. With each successive generation of smart balloon, lighter and more power-efficient instruments are sought and implemented, so that an increasingly diverse set of in situ observations can be made, while still adhering to weight/energy restrictions.

LAGRANGIAN BALLOON DEVELOPMENT AND DEPLOYMENT. *ASTEX/MAGE.* The ASTEX/MAGE field experiment was held in the vicinity of the Azores Islands in June 1992 to study the relationship between marine chemistry, aerosols, and clouds, and air–sea exchange (Albrecht et al. 1995; Huebert et al. 1996a). Understanding the evolution of marine boundary layer (MBL) clouds, a primary goal of ASTEX/MAGE, is critical in weather and climate prediction, in part because of their significant impact on the Earth's radiation budget. Two sets of six constant-level balloons (1.6 m^2 tetroons) were deployed from the *Oceanus* research vessel during the two intensive Lagrangian experiments (Fig. 2) (Businger et al. 1996).

The first-generation ASTEX/MAGE tetroon was a simple constant-level balloon made of a single shell of Mylar, with a tetrahedral shape for ease of construction, that carried only a GPS receiver from Magellan Systems for position data (Fig. 3a, appendix). The GPS receiver was suspended in an external payload beneath the tetroons, which had a maximum altitude of ~1500 m. An advantage of the small tetroon design is its economy, allowing multiple tetroons to be staged and released at one time (Fig. 2). An inexpensive and unmodified ultra-high-frequency radio transmitter and modem transmitted balloon position data to nearby aircraft. A single transmission frequency served all transponders. Time data from GPS receivers were used to keep the transponder transmissions synchronized, thus allowing transmissions from multiple tetroons to be scheduled to avoid interference.

The tetroons were ballasted to attain a mid–boundary layer flight level of 500–750 m above sea level, which was sufficiently below the boundary layer inversion to avoid ejection into the free atmosphere by penetrative convection, and at a level near that

[2] Federal Aviation Administration Regulations Part 101, Subpart D—Unmanned Free Balloons; go to www.faa.gov/ for more information.

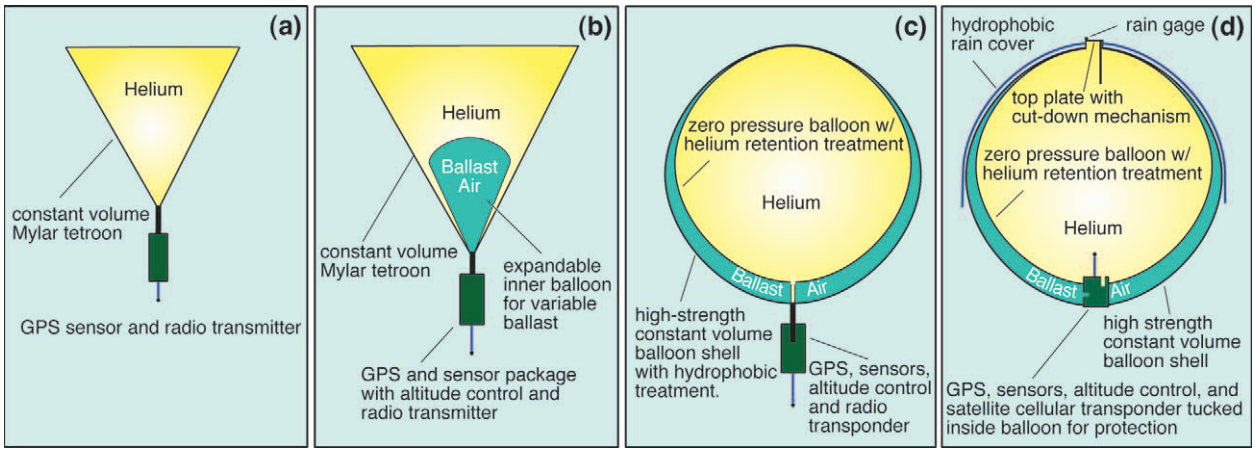

Fig. 3. Schematic diagrams showing primary components of four generations of NOAA balloons deployed in (a) ASTEX/MAGE, (b) ACE-1, (c) ACE-2, and (d) ICARTT.

of the mean vertically averaged horizontal velocity, as discerned from shipboard radiosondes. At the time of the ASTEX/MAGE experiments, the GPS constellation was sufficient to provide continuous latitude and longitude information, but occasionally only three satellites were in view, preventing the receiver from supplying continuous balloon elevation data. During those periods, a constant altitude was assumed.

The Lagrangian strategy was applied by following a column of air of an order of 50 km in diameter to study the evolution of vertical structure and clouds in the MBL as the air mass advected from cold to warm water in the trade winds (Fig. 4). Data collected by the GPS receivers on the tetroons and by instruments aboard two C130 Hercules research aircraft were used to calculate estimates of the entrainment rate, time-dependent horizontal divergence, cumulus mass flux, internal mixing time, and entrainment dilution time for the MBL during the two Lagrangian studies (Bretherton and Pincus 1995; Bretherton et al. 1995b). Estimation of the entrainment rate is a key component of chemical or thermodynamic budget studies of the MBL. Bretherton et al. (1995a) use data taken during ASTEX/MAGE to show that moisture structure in the upper part of the MBL can be used as a predictor of low-cloud fraction. ASTEX Lagrangian data continue to be valuable in validating numerical modeling of the MBL (e.g., De Laat and Duynkerke 1998; Sigg and Svensson 2004).

A number of chemical evolution papers of note resulted from the ASTEX Lagrangian experiments (including Blomquist et al. 1996; Noone et al. 1996; Wingenter et al. 1996; Zhuang and Huebert 1996; Huebert et al. 1996b; Clarke et al. 1996; Jensen et al. 1996). MBL budgets for sulfur dioxide and dimethylsulfide (DMS) in the MBL were examined (Blomquist et al. 1996) during the two Lagrangian experiments. The observed overnight increase in DMS and the predicted increase based on a budget analysis (using a simple surface flux model) agree within the precision of the data for the first Lagrangian experiment.

Zhuang and Huebert (1996) made repeated measurements of ammonium aerosol in a European air mass as it passed over the North Atlantic Ocean near the Azores during the second Lagrangian experiment. Their aircraft observations show that ammonium concentrations stayed relatively constant, in spite of dilution by low-ammonia free-tropospheric air, implying that the North Atlantic was emitting ammonia vapor, a conclusion that is supported by ship observations (Huebert et al. 1996b). These results suggest that the atmosphere may redistribute marine ammonia over hundreds or thousands of kilometers by vapor emission, conversion to aerosols, and deposition in rainfall.

Clarke et al. (1996) studied the evolution of aerosol populations in several layers during the second Lagrangian, quantifying the impacts of mixing, coagulation, and removal on aerosol properties. The observations show that airmass boundaries can be very sharp and they document mesoscale variability in the aerosol population within an air mass.

The results of the studies that capitalized on data collected during the ASTEX/MAGE Lagrangian experiments were made possible in large part by the tetroon GPS position data, which allowed U.S. and U.K. research aircraft to repeatedly sample the MBL air in the vicinity of the drifting balloons (Fig. 4). Divergence calculated from tetroon position data provided a valuable independent measure of entrainment for researchers. A drawback of the

simple ASTEX/MAGE tetroon design, however, was the lack of ability to compensate for the impact of precipitation loading and radiation on the buoyancy of the tetroons (Fig. 3a). This deficiency was particularly evident in the performance of the six tetroons released during the first Lagrangian experiment when moderate drizzle caused all six tetroons to sink to the ocean surface after only six hours of flight (see Fig. 4b in Businger et al. 1996). The early tetroons did not carry any sensors to measure atmospheric variables, such as pressure, temperature, and relative humidity. Pressure data, in particular, would have been useful to estimate tetroon altitudes at a time when the GPS satellite network was incomplete.

ACE-1. The second-generation design of Lagrangian marker tetroons included control of balloon lift through the action of a pump-and-release valve on an internal pressurized ballast bladder, allowing the tetroon buoyancy to be adjusted by the onboard computer when the tetroon traveled vertically outside a range of altitudes set prior to release (Fig. 3b) (Businger et al. 1999). The tetroons were deployed in clean air in the vicinity of Tasmania, Australia (Fig. 4), in December 1995, in two Lagrangian (A and B) experiments during ACE-1 (Bates et al. 1998). In addition to the GPS location obtained by a MicroTracker onboard from Rockwell, the ACE-1 tetroons provided barometric pressure, air temperature, relative humidity, and tetroon status data (appendix). At the time of the ACE-2 field experiments, the GPS satellite constellation was fully operational; however, in a practice referred to as *selective availability,* the military intentionally degraded the accuracy of civilian GPS receivers. Running means of the position data were calculated and pressure data from the tetroon sensor were used to mitigate the impact of selective availability. President Clinton ordered the termination of selective availability on 1 May 2000.

In addition to providing GPS position data for the Lagrangian strategy, meteorological data collected by the tetroons (appendix) were directly utilized in a number of the studies (e.g., Wang et al. 1999a,b; Russell et al. 1998; Suhre et al. 1998). A novel pattern was flown by the National Center for Atmospheric Research (NCAR) C-130 research aircraft during the Lagrangian experiments in which a series of nearly circular loops were flown, with each loop centered approximately on the drifting tetroon positions (Figs. 5 and 6). Estimates of mesoscale entrainment, vorticity, and divergence were then derived from the flight-level and balloon data (Lenschow et al. 1999).

The boundary layer mean structure and its evolution along the ACE-1 Lagrangian trajectories were investigated using two-dimensional cross-sectional plots of vertical and horizontal (along the balloon trajectory) variation of potential temperature, water vapor, wind components, and ozone concentration (Wang et al. 1999a). The Southern Hemispheric MBL was characterized by a two-layered structure, with contrasting values of potential temperature, water vapor, and ozone concentration observed in

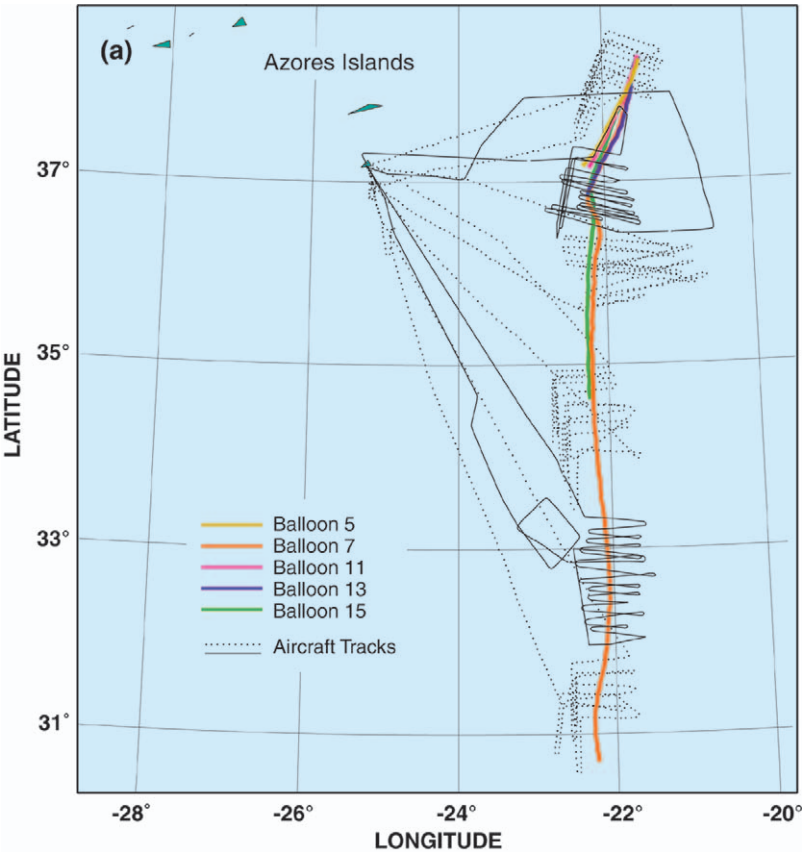

Fig. 4. Research aircraft flight tracks (NCAR C130, thin dashed; U.K. C130, thin solid) and tracks of the marker tetroons during the second ASTEX Lagrangian experiment: 2100 UTC 18 Jun–1200 UTC 20 Jun 1992.

Fig. 5. The NCAR C-130 aircraft rests on the tarmac of the Hobart International Airport, in Tasmania, during ACE-1. When fully fueled, the NCAR C-130 can carry a payload of 13,000 lb, including instruments, scientists, and flight crew.

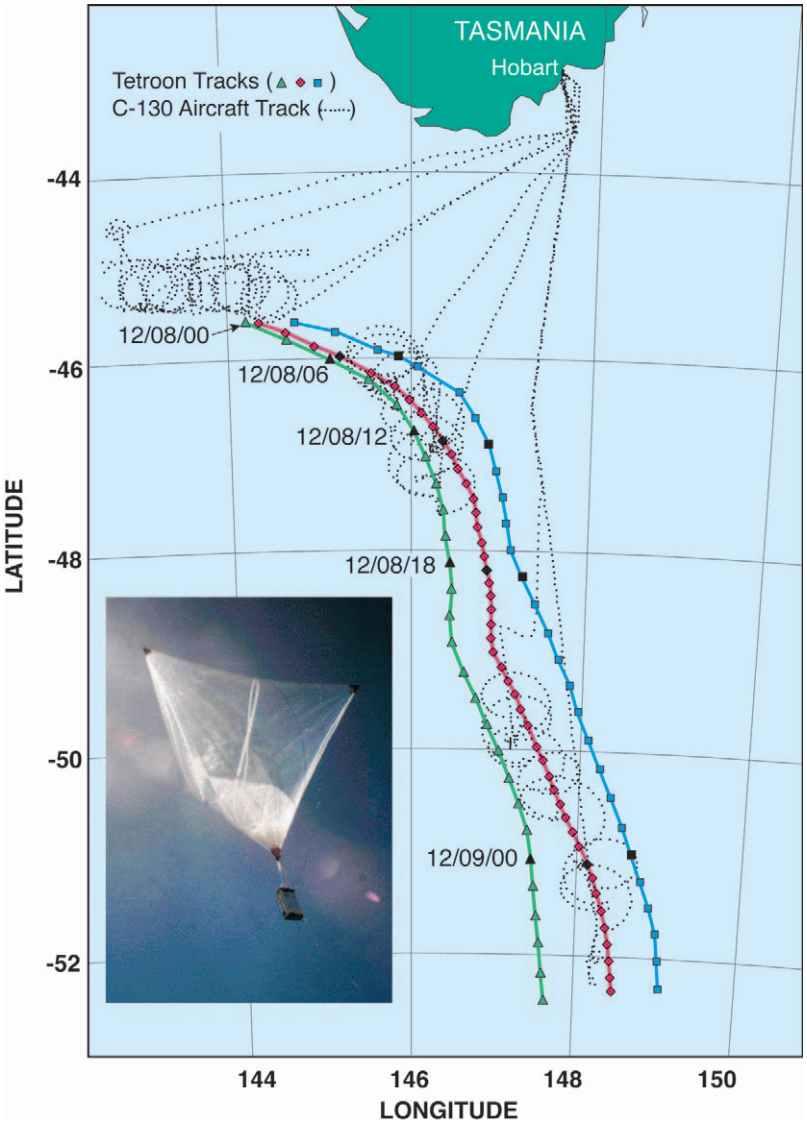

Fig. 6. Tracks of three ACE-1 smart tetroons released on 8 Dec 1995 and C-130 aircraft flight patterns during Lagrangian B. Black symbols indicate tetroon positions at synoptic times (mm/dd/hh) (adapted from Businger et al. 1999). Inset shows photo of the ACE-1 tetroon in flight.

the two layers. A variation in the magnitude of the observed turbulence, and thus in the turbulence mixing in the two layers, helped to explain the observed MBL structure, which included a boundary layer characterized by surface shear-induced turbulence surmounted by a buffer layer below the inversion that included intermittent weak turbulence associated with cumulus clouds (Wang et al. 1999b).

Estimates of the entrainment rate of DMS and aerosol particles between the lower and upper layers during Lagrangian B demonstrated that exchange occurred across the interface between these two layers in both upward and downward directions (Russell et al. 1998). Aircraft observations indicate that aerosol particles were mixing downward into the boundary layer from the buffer layer, while DMS was transported upward. This fortuitous enhancement of aerosol particles in the buffer layer allowed for the simultaneous use of DMS and aerosol particle budgets to track the bidirectional entrainment rates. These estimates were compared to those from measurements of mean vertical motion and boundary layer growth rate, and from estimates of the fluxes and changes in concentration across the layer interface. In addition, three different techniques showed good agreement in the estimation of DMS emission rates from the ocean surface, giving confidence in the entrainment rates.

Suhre et al. (1998) used a one-dimensional Lagrangian model to study the time evolution of gas phase photochemistry during the ACE-1 Lagrangian B experiment. From the combined observational

and modeling work, they conclude that ozone, having a relatively long photochemical lifetime in the clean marine boundary layer, is controlled by vertical transport processes, in particular synoptic-scale subsidence or ascent. Their model-predicted concentrations of peroxides, OH, and DMS are in agreement with observations, both on cloudy and noncloudy days.

Mari et al. (1999) also employed a one-dimensional Lagrangian model to simulate vertical profiles and temporal evolution of DMS, sulfur dioxide, aerosol methane sulfonate, and non–sea salt sulfate that were measured during the three flights of the Lagrangian B experiment. Their model results and the Lagrangian observations suggest that oxidation of sulfur dioxide in sea salt particles appears to be a dominant process and controls the sulfur dioxide lifetime during Lagrangian B.

The addition of variable lift to the ACE-1 design enabled the tetroons to compensate for almost all atmospheric conditions. The exception was when precipitation or condensation accumulated on the tetroons' flat upper surface, causing the tetroons to descend near the surface at night (see Businger et al. 1999, their Fig. 4a). Siems et al. (2000) used model-simulated trajectories to investigate and discuss the impact of the vertical excursions of the ACE-1 tetroons on trajectories in a sheared environment. Their results suggest limitations of the Lagrangian approach under highly sheared conditions, and they reinforce the importance of having good control of the vertical position of the balloons under sheared conditions so that the balloon trajectories reflect the mass-weighted average horizontal velocity in the boundary layer. Another limitation of the ACE-1 tetroon was the fact that one-way radio communication did not allow for operator adjustment of the flight level following the tetroon's release.

ACE-2. Significant design improvements were incorporated into the third-generation Lagrangian balloon (Fig. 3c, appendix), which was deployed during the ACE-2 field program conducted between the coast of Portugal and the Canary Islands from 16 June through 26 July 1997 (Fig. 7a) (Johnson et al. 1998; Johnson et al. 2000a,b,c). These improvements include i) a spherical design to reduce precipitation

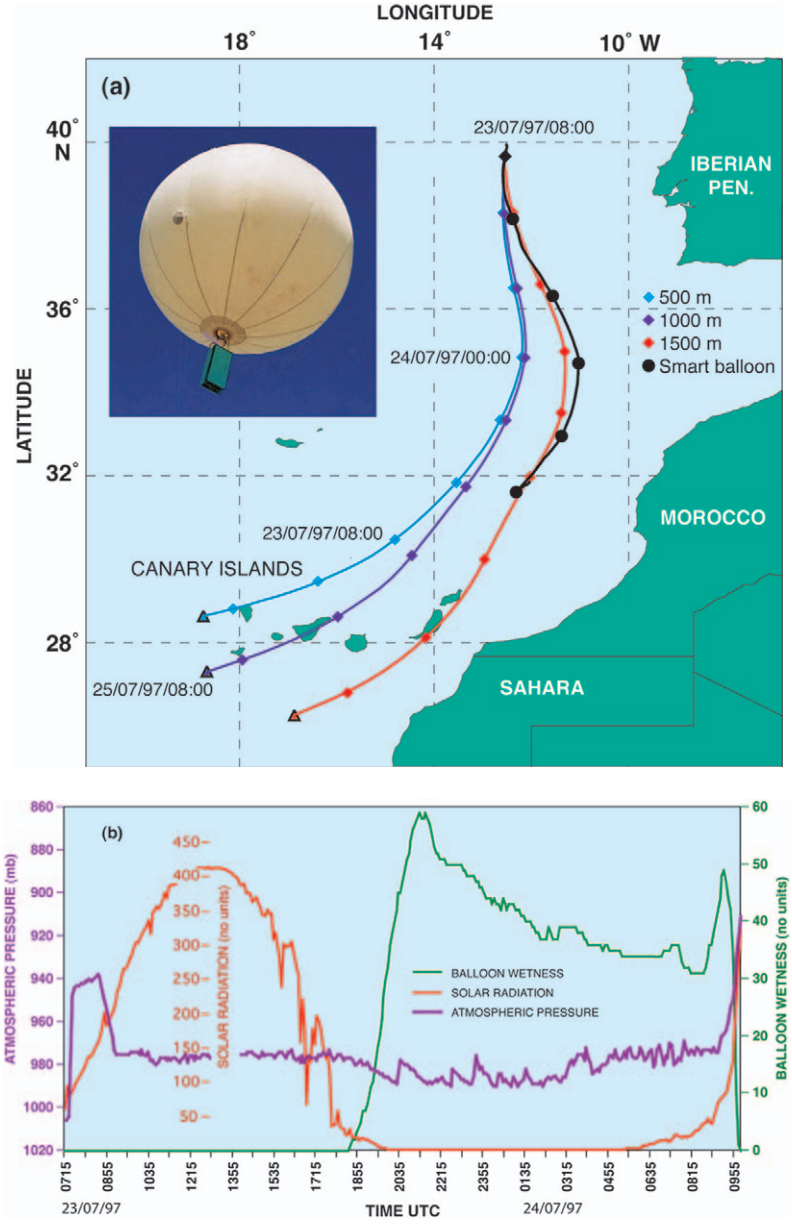

Fig. 7. (a) ACE-2 Lagrangian 3 with smart balloon track (black) and NCEP global spectral model trajectories for 500 (red), 1000 (purple), and 1500 (blue) m with date and UTC time labels. Inset shows photo of the ACE-2 balloon in flight. (b) Time series of pressure (mb), balloon wetness, and solar radiation (no units) from ACE-2 Lagrangian smart balloon, starting at 0715 UTC 23 Jul 1997 and continuing until 1000 UTC 24 Jul 1997 (adapted from Johnson et al. 2000c).

loading, ii) two-way communication with the balloon to allow for interactive control of the balloon-operating parameters by an operator, and iii) a stronger outer shell made of Spectra that was able to withstand the internal superpressure needed to significantly increase the balloon's dynamic lift range. In addition to the variables transmitted by the ACE-1 tetroon, the ACE-2 balloon provided internal balloon temperature and superpressure, and ambient solar radiation data.

One of the primary aims of ACE-2 was to quantify the physical and chemical processes affecting the evolution of the major aerosol types over the North Atlantic (Raes et al. 2000). To this end, three cloudy Lagrangian experiments were conducted during the ACE-2 field program (Johnson et al. 2000a). Of the three ACE-2 Lagrangian experiments, the first was conducted in clean air, whereas the second and third were conducted in polluted air emanating from the European continent. A close connection was observed between meteorological factors (such as horizontal and vertical wind speed, boundary layer development, entrainment, and humidity fields) and aerosol and cloud characteristics (Raes et al. 2000; Sollazzo et al. 2000).

A detailed time-scale analysis of observed aerosol size distribution during the clean first Lagrangian suggests that the dominant loss process for fine-mode aerosol is coagulation, while the enhancement of accumulation-mode aerosol can be almost totally attributed to an enhanced sea salt aerosol flux into the reduced mixed layer volume (Hoell et al. 2000; Johnson et al. 2000a). The sulfur cycle in this air mass could be explained by the emission of DMS from the sea surface (Andreae et al. 2000).

During the second Lagrangian, observations and model simulations suggest that the primary factors relating to reduced aerosol concentrations were dilution with cleaner free-tropospheric air and in-cloud chemical reactions (Hoell et al. 2000; Dore et al. 2000; Andreae et al. 2000). Thermodynamic changes within the boundary layer included decoupling due to an increasing sea surface temperature and a change in the subsidence rate in the free troposphere. Sulfur dioxide was removed rapidly with lifetimes on the order of half a day in cloud-topped boundary layers (Andreae et al. 2000).

Very little change in aerosol characteristics was measured during the third ACE-2 Lagrangian (Fig. 7), where the pollution in the MBL was continually being replenished by entraining residual continental air from a decoupled boundary layer above (Wood et al. 2000). The decoupled polluted layer between the MBL and the unpolluted free troposphere was only weakly and intermittently turbulent, preventing significant entrainment of clean air into the polluted layer from aloft. These observations have important implications for the rate at which polluted continental air is transformed into clean marine air.

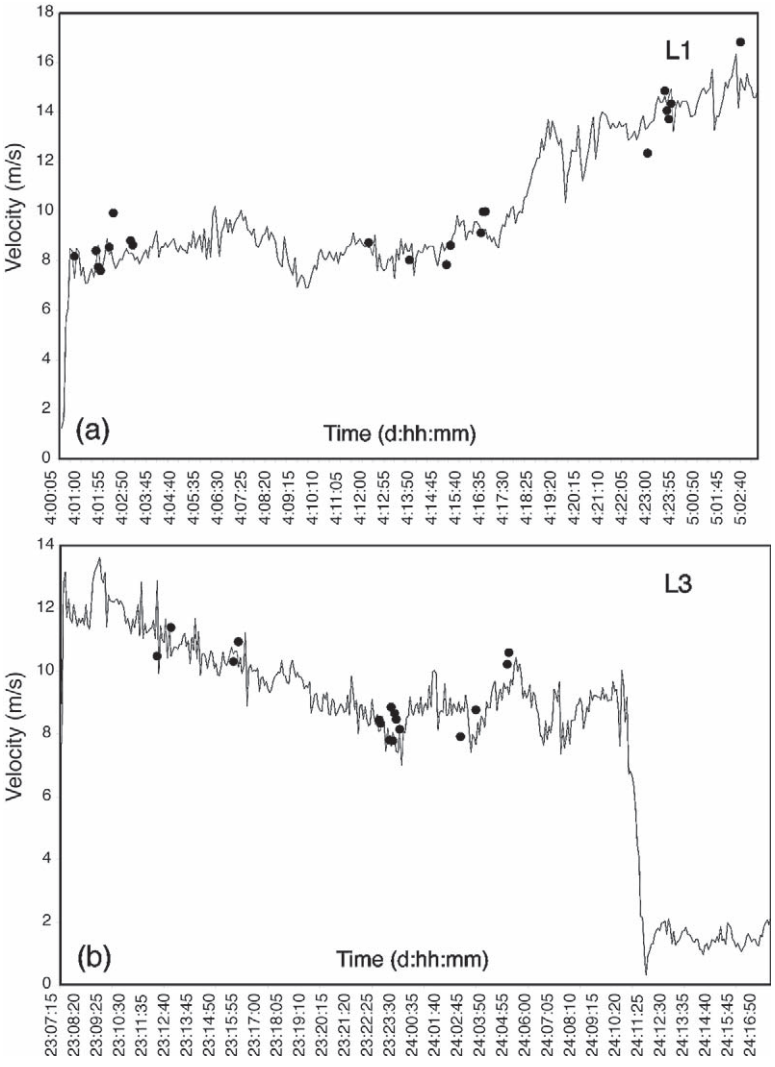

Fig. 8. Comparison of smart balloon velocity (line) to C-130 aircraft flight-level wind speed (m s^{-1}) for Lagrangian 1 (balloon 2) and Lagrangian 3 (balloon 8) (adapted from Johnson et al. 2000).

The ACE-2 balloon proved very successful in maintaining altitude despite condensation loading and radiational effects (Fig. 7b). The stronger balloon shell provided an order of magnitude increase in the dynamic lift range over the ACE-1 design, and the spherical design reduced the collection of liquid water. The altitude control worked during night and day even when the wetness sensor showed condensation on the surface of the balloon. Comparisons between the balloon velocity and proximate C-130 flight-level wind data show that the differences were smaller than the errors associated with the wind measurements themselves, lending confidence to the assertion that the balloons travel with the speed of the air in which they are embedded (Fig. 8).

A SMART BALLOON FLIGHT FOR THE RECORD BOOKS. Advances in technology utilized in the fourth-generation smart balloon dramatically increased the autonomous range and in situ measurement capabilities of these balloons when they were deployed during the ICARTT field program (Fig. 9). The improvements included i) satellite communications that replaced the point-to-point radio system and eliminated the need for an aircraft to be in close proximity to receive the balloon data (Fig. 10a); ii) balloon design that included an airtight fiberglass cylindrical compartment to hold the sensors and transponder inside the balloon shell to provide protection and added stability from wind, rain, turbulence, and possible ocean surface encounters (Fig. 3d); iii) solar power (Fig. 10b); iv) an innovative lightweight ozone sensor; and v) improved meteorological sensors (appendix).

Like its predecessor the ICARRT balloon had a high strength and durable outer shell constructed of Spectra fabric, and it included two inner bladders—the outer bladder was filled with pressurized ambient air and the inner bladder with helium. The volume enclosed by the Spectra shell increased from 12.9 to 16.4 m^3, providing the dynamic lift needed to allow the balloon to compensate for precipitation rates of up to 7.6 cm h^{-1}, a highly desirable ability for flight durations from days to weeks at a low altitude (< 3.5 km). As in the previous design, balloon altitude is controlled by using a pump to move air in/out of the pressurized air bladder to effectively increase/decrease its buoyancy. The ability to both remotely and autonomously control the ascent/descent timing and rate combined with an ever-expanding measurement capability has significantly extended the range of applications of this NOAA smart balloon for atmospheric research (Fig. 11).

An Iridium satellite data modem model A3LA-I allowed continuous communication with the smart balloon during the ICARTT flights (Fig. 10a). Balloon position was provided by a miniature Lassen SQ GPS manufactured by Trimble Navigation. Onboard sensors included a Vaisala model PTB101B for pressure and a Vaisala model HMP45C temperature–relative humidity probe, and an Apogee Instrument, Inc., Infrared Temperature Sensor (IRTS-S) was used to determine IR surface temperature. A miniature precipitation gauge was also mounted on the top plate of the balloon. See the appendix for additional details.

Lithium ion batteries coupled with three flexible solar cells mounted on top of the balloon provided electrical power (Fig. 10b). The solar panels were 25 cm × 71 cm and weighed 56 g each. Total available battery power was about 91 W h. The length of time for which the batteries and solar cells could keep the balloon functioning depends on weather conditions, pump-operating time, and data-gathering frequency.

Fig. 9. NOAA's Randy Johnson, balloon engineer and designer, checks the superpressure of a smart balloon during ICARTT.

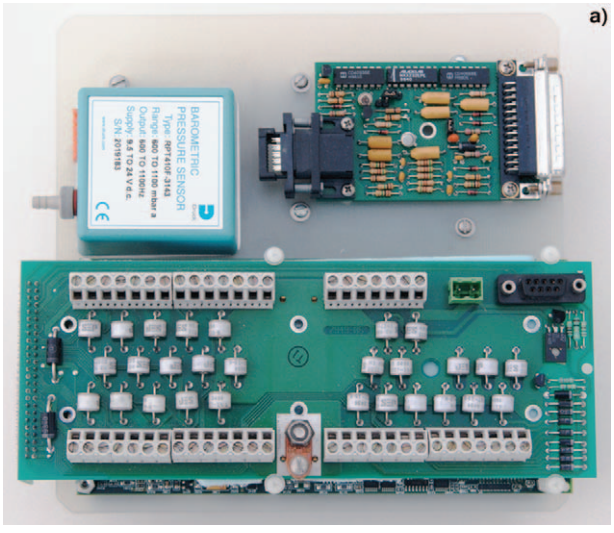

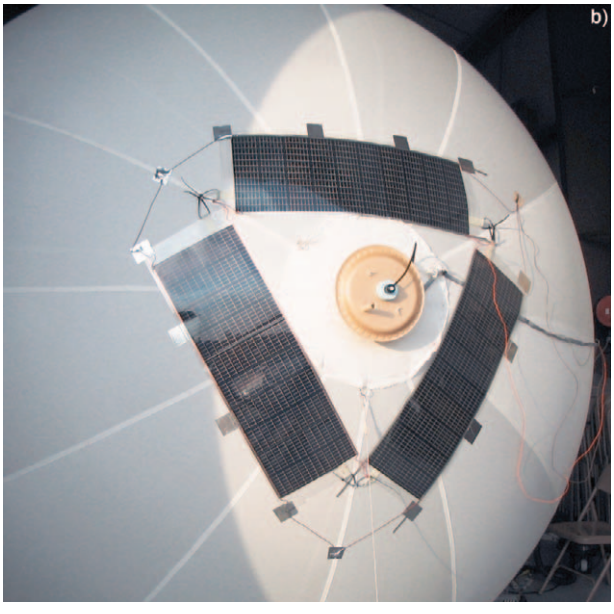

Fig. 10. (a) Transponder package with microcontroller, the Druck barometric pressure sensor, and the Iridium modem interface board. The GPS receiver–antenna, temperature, IR temperature, and Iridium antenna are outside the package. (b) Power from the solar panels is routed via separate wires to the lithium ion batteries attached to the lower portion of the balloon.

Four smart balloons, specially instrumented with new lightweight ozone sensors, were released from the northern tip of Long Island, New York, during the ICARTT campaign conducted over the northeastern United States and the North Atlantic Ocean during July and August 2004 (Fig. 11). The release site was chosen for its rural coastal location away from air traffic lanes, yet proximate to the source regions for East Coast pollution plumes. During two balloon flights the NOAA WP3-D research aircraft intercepted the balloons, with both measuring the same values of ozone. The balloons also served as a marker for the plumes, facilitating their repeated sampling by aircraft over a two-day period.

Immediately after release, each of the balloons was lofted to 500 m where they sampled the New York City urban plumes as indicated by ozone mixing ratios exceeding 100 ppbv and peaking at 185 ppbv. The first two balloon flights lasted 21 and 49 h, respectively. Both flights were terminated as a result of loss of buoyancy. The first balloon was recovered in northern Maine and redeployed as balloon 4.

Over the remote Atlantic Ocean, aircraft and balloon observations suggest that the 500–3500-m column was largely fumigated, with polluted continental outflow concentrated in layers on the order from tens to hundreds of meters thick (Talbot et al. 2006; Mao et al. 2006). Peak ozone mixing ratios of 160 ppbv were observed numerous times many thousands of kilometers from the North American source region. Balloon 4's flight was terminated when its battery began to fail over the central North Atlantic (Fig. 11).

Balloon 3 completed a transatlantic flight in the vicinity of northern Africa, which marked the first time a low-level balloon drifted across the Atlantic Ocean from North America to Africa and continuously measured ozone and meteorological conditions (Figs. 11 and 12). Our data suggest that a portion of the New York City urban plume may have traveled nearly 7,000 km over a 2-week interval while remaining intact enough to maintain levels of ozone similar to that which we observed just downwind of North America (Talbot et al. 2006; Mao et al. 2006). These unique observations demonstrate an effective low-cost option for future observing strategies in remote regions of the atmosphere. Data from the ICARTT balloons are actively being analyzed at this writing.

The development and subsequent integration of the University of New Hampshire's mini-O_3 sensor into the smart balloon package proceeded on a one-year accelerated pace for the ICARTT campaign. Consequently, several compromises were made in the integration of supporting meteorological sensors. The most notable compromise was the elimination of the aspiration shield for the temperature probe in order to accommodate the inlet for the ozone sensor, resulting in morning and afternoon temperature peaks caused by solar heating of the instrument package with each sunrise and sunset. Figure 12 shows plots of the raw data transmitted by the balloon and includes times of suspect observations to

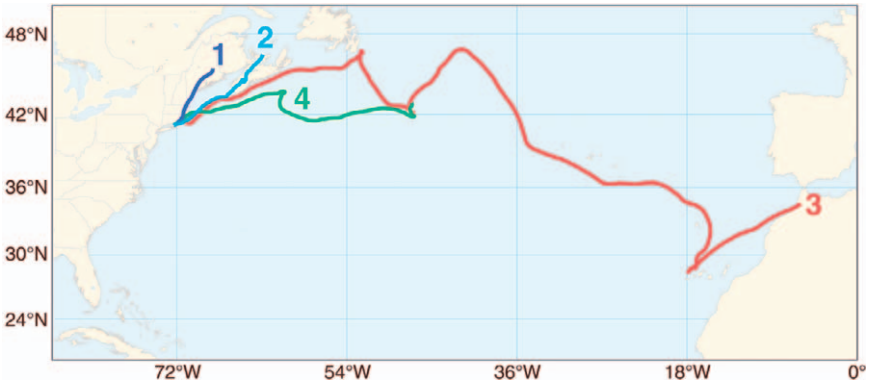

Fig. 11. Tracks of four smart balloons (labeled) released during the ICARTT field experiment held in the summer of 2004.

give the reader an example of the quality control that must be performed postexperiment. In addition to evidence of solar contamination in the temperature time series, ozone observations on 8 August appear contaminated by rainwater.

On several occasions during ICARRT the smart balloons were raised above low-level clouds to allow their battery packs to recharge. The pressure trace in Fig. 12 indicates such a change in altitude for balloon 3 on 8 August. On 13 August a decision was made to increase the ballast air in balloon 3 to bring it down to the ocean surface for safety reasons. However, in a fluke of geography and winds, it struck Las Palmas in the Canary Islands where the outer ballast bladder was punctured, after which the balloon promptly rose to near 800 mb. Some of the instruments, such as the pyranometer and the solar cells, failed upon impact. The batteries subsequently depleted until communication with the balloon ceased on 15 August.

DEVELOPMENT OF A HURRICANE BALLOON. In an environment where it is challenging to obtain in-situ data, hurricane balloons promise to provide data on the thermodynamic history and trajectories of air parcels to better characterize the evolution of the energy content of the marine boundary-layer inflow to hurricanes and its relationship with changes in hurricane intensity (Fig. 13). GPS position and thermodynamic data can be analyzed for evidence of the presence of organized eddies and their influence on the surface fluxes into the inflow layer (e.g., Morrison et al. 2005; Foster 2005). A Lagrangian experiment complements the essentially Eulerian experiments carried out during routine NOAA aircraft reconnaissance missions, and capitalizes on the availability of new high-resolution GPS dropwindsondes, turbulent flux sensors, and the Doppler radar on the NOAA WP-3D aircraft.

Two attempts have been made to intercept a hurricane with a smart balloon. The first attempt was made on 25 October 2002 when a prototype hurricane balloon was released from a weather station in Mazatlan, Mexico, into the inflow of Hurricane Kenna (appendix). A Pacific storm was chosen for this early test because there was hesitancy on the part of some Air Force reconnaissance pilots to fly with an "untested" balloon. President G. W. Bush was at a

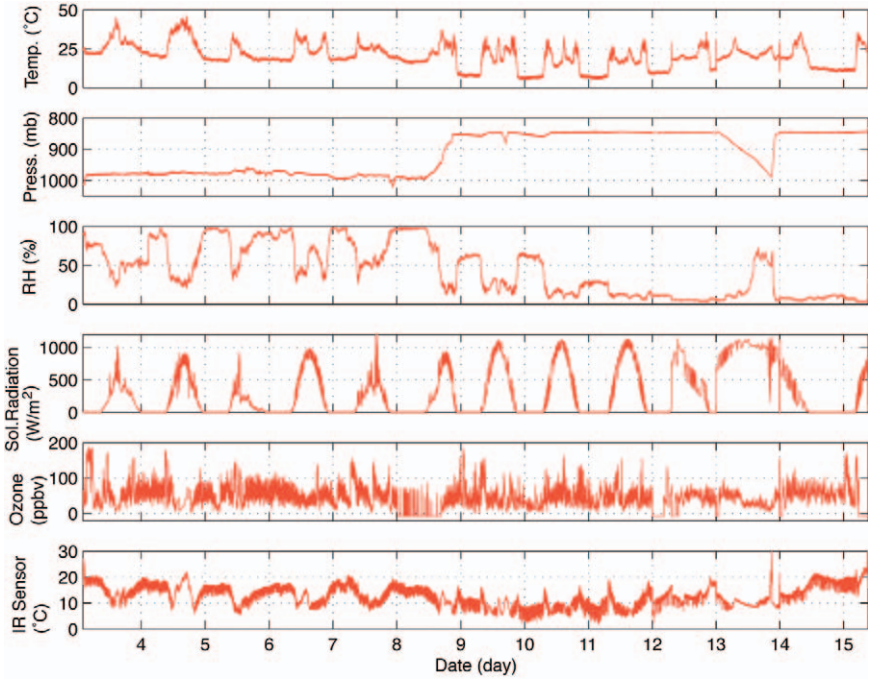

Fig. 12. Time series data plotted for smart balloon 3, including ambient air temperature, barometric pressure, relative humidity, solar radiation, ozone, and downward-looking infrared temperature. See balloon 3 track in Fig. 11. See text for additional explanation.

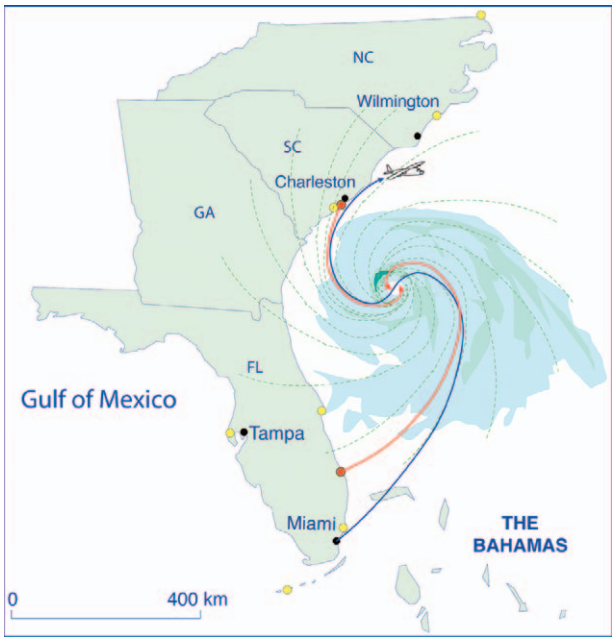

Fig. 13. Idealized schematic showing tracks of two hurricane balloons (red lines) deployed in a Lagrangian energetics experiment. Blue line shows flight path of research aircraft with dropsondes.

meeting in Baja California at this time, and perhaps ironically a reconnaissance aircraft was deployed into Hurricane Kenna. The Hurricane Kenna balloon was actually the first to have its instruments and transponder placed in a fiberglass cylinder and tucked into the durable Spectra shell of the balloon for protection from the storm elements. Roughly 40 minutes into the flight the balloon abruptly began to rise from ~1 km in the inflow layer to nearly 3 km and into the hurricane's outflow. The wind direction changed almost 180° in the process, returning the balloon to the vicinity of Mazatlan, where it was brought down using a cut-down mechanism designed to provide added safety to reconnaissance crews. Although the Kenna balloon did not succeed in intercepting the storm because of the ballast bladder failure, all of the other systems and instruments worked flawlessly. Significantly, the exercise also demonstrated that the balloon team could overcome the significant logistical obstacles of timing travel to a foreign country, based on a hurricane-track forecast, to stage and release a balloon at just the right time to intercept the hurricane.

During the historical 2005 hurricane season, the NOAA balloon team went to Puerto Rico for an ill-timed two-week window (just between Hurricanes Katrina and Rita). Two NOAA hurricane balloons were staged and released from the Coast Guard Air Station Borinquen located on the northeast coast of Puerto Rico in an effort to intercept Hurricane Ophelia as part of RAINEX (appendix). The solar panel circuit failed on the first balloon and the balloon was terminated prior to reaching Hurricane Ophelia, which, at quite a distance from Puerto Rico, was approaching the coast of the Carolinas. The second RAINEX balloon, released ~4 hours after the first, did not find a favorable northward-directed airstream and instead tracked westward. After a little more than three days of flight the balloon suffered a communication failure, essentially due to friendly fire; the Iridium satellite phone, obtained through the military, was rendered mute by a military security protocol of which the investigators were not aware. Data from these balloon flights, neither of which intercepted its hurricane target, are still being analyzed.

SUMMARY AND CONCLUSIONS. This paper provides an overview of four generations of Lagrangian smart balloon development at NOAA ARLFRD, and reviews the scientific insights that have been gained from a series of Lagrangian field experiments that employed these balloons as airmass markers. The capability of the Lagrangian balloons has been extended with each successive generation. Starting with small ASTEX tetroons, which provided only GPS position data via a radio transmitter, the fourth-generation ICARTT smart balloon has evolved into a sophisticated in situ instrument platform that transmits a growing suite of measurements globally via satellite cellular telephone, and whose buoyancy can be controlled to offset even heavy rain. The third smart balloon released from Long Island during ICARTT made a trans-Atlantic crossing in the lower troposphere, passing the coast of Morocco after an unprecedented 12 days of 10-s-averaged data collection and transmission (Figs. 11 and 12).

A number of research papers have presented detailed results derived from the Lagrangian field experiments. As a consequence of this body of work, our understanding of the structure and dynamics of the MBL and its role in the evolution of gaseous and aerosol components of clean and polluted air masses has advanced.

Despite successful results emerging from Lagrangian field experiments in specific cases, a number of studies also noted difficulties in coming to quantitative conclusions based on uncertainties in the datasets. Therefore, it is important to stress the challenges associated with carrying out successful

Lagrangian field experiments. The ability to resolve the effects of separate processes influencing both gas and aerosol during Lagrangian evolution depend on i) an adequate assessment of the variability in the air mass, ii) the ability to characterize this variability relative to the uncertainties in resampling the air mass, and iii) the extent to which the substantial changes due to entrainment alone can be determined reliably. However, difficulties encountered in the interpretation of Lagrangian results should be a sobering lesson for the interpretation of Eulerian experiments, where advection presents an even more serious complicating factor.

By steadily and incrementally improving the technology for undertaking Lagrangian studies, we have reached a point where unique and valuable insights are being derived from this observational strategy. As we implement further improvements to this strategy, for example, by using chemical transport models to predict locations where species of interest will undergo the most rapid change, the error bars will continue to shrink and more process rates will be amenable to measurement.

The NOAA smart balloon design provides a field-proven autonomous Lagrangian platform that is capable of flight durations ranging from a few hours to a few weeks. The dynamic range afforded by the high-strength spherical shell and the lift control in the ICARTT design allow the balloons to remain within desired altitude-operating limits despite the impacts of condensation, rainfall, and radiative cooling. The growing suite of lightweight instruments borne by smart balloons provides expanding opportunities for the collection of in situ and remotely sensed data. The in situ data combined with the balloon's dynamic range enable the balloon transponder to be programmed to remain at a constant altitude, to follow an isobaric or isentropic surface, or to perform vertical soundings. With the availability of satellite data telemetry, the balloon flight can be remotely controlled and the data downloaded anywhere on the globe, eliminating the need for proximate aircraft. These capabilities and the economical cost of the design (< $8,000 each for materials) make the smart balloon an attractive platform for a broad range of future applications in atmospheric research.

Future deployment. A series of NOAA smart balloon experiments is planned during the next few years, including deployment in the second TexAQS during summer 2006 (appendix) and as a part of a Lagrangian experimental strategy to study hurricanes. At this time the sensor integration and instrument issues identified during ICARRT and RAINEX have been addressed. A new fiberglass transponder tube has been designed and constructed to hold all components of the transponder, communications systems, and environmental sensors in a single enclosure with a 20-cm inner diameter. Potential failure points in the balloon bladders have been reviewed and addressed in the redesign. A miniature pulse output-type rain gauge has been developed to improve balloon precipitation measurement. As a droplet moves past a small funnel and between an infrared light-emitting diode and infrared sensor, it refracts the beam, causing a pulse at the sensor. Tests indicate that a droplet volume formed in this manner varies by only about 3% for precipitation rates ranging from 0.2 to 30 cm h^{-1}.

A real-time Web display of the balloon track and the raw data output have been completed, allowing interested parties to track the balloon position, altitude, and ozone levels in real time at any time during a balloon flight. This facility is particularly important in hurricane studies in that it allows research aircraft pilots to intercept (or avoid) the balloons, and also for educational purposes by motivating students to follow the progress of a hurricane balloon toward an eyewall.

Given the logistics of staging smart balloons (they require a hangar with a large ~3.5 m door) and the cost of their construction and deployment, the number of balloons released at one time will remain limited (about one to three balloons), given the current levels of support. Successful releases into tropical cyclones may lead to an opportunity to release greater numbers of hurricane balloons into diverse inflows around storms in the future.

ACKNOWLEDGMENTS. We are grateful to Shane Beard for assistance in the field. Roger Carter provided programming support for the transponder design. Donald Troop played a major role in the design and implementation of the miniature ozone sensor during ICARTT. We are grateful to Nancy Hulbirt for her contribution to the graphics. In particular, Dr. Businger is grateful to Professor B. Huebert for a pivotal introduction to Ray Dickson at ARLFRD in 1990, and for his constructive review of an early draft of this paper. Constructive reviews were also provided by Dr. J. K. Angell, Dr. K. L. Clawson, Dr. W. Schack III, and anonymous reviewers. This research was supported by the National Science Foundation under Grant ATM99-09011 and the NOAA Targeted Wind Sensing program under Grants NA03OAR460163 and NA04OAR4600157.

APPENDIX. Evolution of the NOAA smart balloon platform technology and capabilities.

Year	1992	1995	1997	2002	2004	2005	2006
Deployment in field experiments	ASTEX/MAGE	ACE-1	ACE-2		ICARRT	RAINEX	TexAQS II
Volume of balloon (m^3)	1.6	4.6	12.9	16.4	16.4	18.8	18.8
Balloon material	Mylar	Mylar	Spectra	Spectra	Spectra	Spectra	Spectra
Shape of balloon	Tetroon	Tetroon	Sphere	Sphere	Sphere	Sphere	Sphere
External/internal payload	External	External	External	Internal	Internal	Both	Internal
Maximum altitude (m)	1500	1000	3100	3300	3500	3500	3200
Battery type	Lithium	Lithium	Lithium	Lithium ion	Lithium ion	Lithium ion	Lithium ion
Solar charger	No	No	No	No	Yes	Yes	Yes
Battery life	36	36	40	24	Indefinite*	Indefinite*	Indefinite*
Communications	Radio	Radio	Two-way radio	Globalstar	Iridium	Iridium	Iridium
Payload weight (kg)	0.7	1.8	2.5	4.7	4.8	4.9	5.1
Instruments	GPS	GPS	GPS	GPS	GPS	GPS	GPS
		Temperature, wetness, barometric pressure, balloon pressure, relative humidity	Temperature, wetness, barometric pressure, balloon pressure, relative humidity, solar radiation,	Temperature, wetness, barometric pressure, balloon pressure, relative humidity, solar radiation, IR temperature, solar panel	Temperature, wetness, barometric pressure, balloon pressure, relative humidity, solar radiation, IR temperature, solar panel, helium pressure, ozone	Temperature, wetness, barometric pressure balloon pressure, relative humidity, solar radiation, IR temperature, solar panel, helium pressure, ozone	Temperature, wetness, barometric pressure, balloon pressure, relative humidity, solar radiation, IR temperature, solar panel, helium pressure, ozone

*From 24 hours to indefinite, given sufficient solar radiation to keep batteries charged. Reduced capability, infrequent communications, high-altitude operation, or other techniques can extend battery life.

REFERENCES

Albrecht, B. A., C. S. Bretherton, D. W. Johnson, W. H. Schubert, and A. Shelby Frisch, 1995: The Atlantic Stratocumulus Transition Experiment—ASTEX. *Bull. Amer. Metor. Soc.,* **76,** 889–904.

Andreae, M. O., W. Elbert, R. Gabriel, D. W. Johnson, S. Osborne, and R. Wood, 2000: Soluble ion chemistry of the atmospheric aerosol and SO_2 concentrations over the eastern North Atlantic during ACE2. *Tellus,* **52B,** 1066–1087.

Angell, J. K., 1974: Lagrangian-Eulerian time-scale relationship estimated from constant volume balloon flights past a tall tower. *Adv. Geophys.,* **18A,** 419–431.

——, 1975: The use of tetroons for probing the atmospheric boundary layer. *Atmos. Technol.,* **7,** 38–43.

——, W. H. Hoecker, C. R. Dickson, and D. H. Pack, 1973: Urban influence on a strong daytime air flow as determined from tetroon flights. *J. Appl. Meteor.,* **12,** 924–936.

Bates, T. S., B. J. Huebert, J. L. Gras, F. B. Griffiths, and P. A. Durkee, 1998: The International Global Atmospheric Chemistry (IAC) Project's First Aerosol Characterization Experiment (ACE-1)—Overview. *J. Geophpys. Res.,* **103,** 16 297–16 318.

Blomquist, B. W., A. R. Bandy, and D. C. Thornton, 1996: Sulfur gas measurements in the eastern North Atlantic Ocean during the Atlantic Stratocumulus Transition Experiment/Marine Aerosol and Gas Exchange. *J. Geophys. Res.,* **101,** 4377–4392.

Bretherton, C. S., and R. Pincus, 1995: Cloudiness and marine boundary layer dynamics in the ASTEX Lagrangian experiments. Part I: Synoptic setting and vertical structure. *J. Atmos. Sci.,* **52,** 2707–2723.

——, E. Klinker, A. K. Betts, and J. A. Coakley Jr., 1995a: Comparison of ceilometer, satellite, and synoptic measurements of boundary-layer cloudiness and the ECMWF diagnostic cloud parameterization scheme during ASTEX. *J. Atmos. Sci.,* **52,** 2736–2751.

——, P. Austin, and S. T. Siems, 1995b: Cloudiness and marine boundary layer dynamics in the ASTEX Lagrangian experiments. Part II: Cloudiness, drizzle, surface fluxes and entrainment. *J. Atmos. Sci.,* **52,** 2724–2735.

Businger, S., S. R. Chiswell, W. C. Ulmer, and R. Johnson, 1996: Balloons as a Lagrangian measurement platform for atmospheric research. *J. Geophys. Res.,* **101,** 4363–4376.

——, R. Johnson, J. Katzfey, S. Siems, and Q. Wang, 1999: Smart tetroons for Lagrangian air mass tracking during ACE-1. *J. Geophys. Res.,* **104,** 11 709–11 722.

Clarke, A. D., T. Uehara, and J. N. Porter, 1996: Lagrangian evolution of an aerosol column during the Atlantic Stratocumulus Transition Experiment. *J. Geophys. Res.,* **101,** 4351–4362.

De Laat, A. T. J., and P. G. Duynkerke, 1998: Analysis of ASTEX-stratocumulus observational data using a mass-flux approach. *Bound.-Layer Meteor.,* **86,** 63–87.

Dore, A. J., D. W. Johnson, S. R. Osborne, T. W. Choularton, K. N. Bower, M. O. Andreae, and B. J. Bandy, 2000: Evolution of boundary-layer aerosol particles due to in cloud chemical reactions during the 2nd Lagrangian experiment of ACE2. *Tellus,* **52B,** 452–463.

Foster, R. C., 2005: Why rolls are prevalent in the hurricane boundary layer. *J. Atmos. Sci.,* **62,** 2647–2661.

Harrison, D. N., 1957: The use of balloons in meteorology. *J. Inst. Navig.,* **10,** 67–70.

Hoecker, W. H., Jr., 1981: A model for predicting diurnal height variations of quasi-constant-density tetroons. *J. Appl. Meteor.,* **20,** 1095–1104.

Hoell, C., C. D. O'Dowd, S. R. Osborne, and D. W. Johnson, 2000: Time-scale analysis of marine boundary layer aerosol evolution: Lagrangian case studies under clean and polluted cloudy conditions. *Tellus,* **52B,** 423–438.

Huebert, B. J., A. Pszenny, and B. Blomquist, 1996a: The ASTEX/MAGE Experiment. *J. Geophys. Res.,* **101,** 4319–4330.

——, L. Zhuang, S. Howell, K. Noone, and B. Noone, 1996b: Sulfate, nitrate, methanesulfonate, chloride, ammonium, and sodium measurements from ship, island, and aircraft during the ASTEX/MAGE. *J. Geophys. Res.,* **101,** 4413–4424.

Jensen, T. L., S. M. Kreidenweis, Y. Kim, H. Sievering, and A. Pszenny, 1996: Aerosol distributions in the North Atlantic marine boundary layer during Atlantic Stratocumulus Transition Experiment/Marine Aerosol and Gas Exchange. *J. Geophys. Res.,* **101,** 4455–4468.

Johnson, D. W., and Coauthors, 2000a: An overview of the Lagrangian experiments undertaken during the North Atlantic regional Aerosol Characterisation Experiment (ACE-2). *Tellus,* **52B,** 290–320.

——, and Coauthors, 2000b: Observations of the evaluation of the aerosol, cloud, and boundary-layer characteristics during the 1st ACE-2 Lagrangian experiment. *Tellus,* **52B,** 348–374.

Johnson, R., S. Businger, and R. Carter, 1998: Evolution of smart balloon design for Lagrangian air mass tracking. *GPS World,* **9,** 33–38.

——, ——, and A. Baerman, 2000c: Lagrangian air mass tracking with smart balloons during ACE-2. *Tellus,* **52B,** 321–334.

Lenschow, D. H., P. B. Krummel, and S. T. Siems, 1999: Measuring entrainment, divergence and vorticity on the mesoscale from aircraft. *J. Atmos. Oceanic Technol.,* **16,** 1384–1400.

Mao, H., R. Talbot, D. Troop, B. Moore, R. Johnson, and S. Businger, 2006: Smart balloon observations over the North Atlantic: Part II—O_3 data analysis and modeling. *J. Geophys. Res.,* **111,** doi:10.1029/2005JD006507.

Mari, C., K. Suhre, R. Rosset, T. S. Bates, B. J. Huebert, A. R. Bandy, D. C. Thornton, and S. Businger, 1999: One-dimensional modeling of sulfur species during the First Aerosol Characterization Experiment (ACE 1) Lagrangian B. *J. Geophys. Res.,* **104,** 21 733–21 750.

Morrison, I., S. Businger, F. Marks, P. Dodge, and J. A. Businger, 2005: An observational case for the prevalence of roll vortices in the hurricane boundary layer. *J. Atmos. Sci,* **62,** 2662–2673.

Noone, K. J., R. D. Schillawski, G. L. Kok, C. S. Bretherton, and B. J. Huebert, 1996: Ozone in the marine atmosphere observed during the Atlantic Stratocumulus Transition Experiment/Marine Aerosol and Gas Exchange. *J. Geophys. Res.,* **101,** 4485–4500.

Raes, F., T. S. Bates, F. McGovern, and M. Van Liedekerke, 2000: The 2nd Aerosol Characterization Experiment (ACE-2): General overview and main results. *Tellus,* **52B,** 111–125.

Russell, L. M., D. H. Lenschow, K. K. Laursen, P. B. Krummel, S. T. Siems, A. R. Bandy, D. C. Thornton, and T. S. Bates, 1998: Bidirectional mixing in an ACE 1 marine boundary layer overlain by a second turbulent layer. *J. Geophys. Res.,* **103,** 16 411–16 432.

Seinfeld, J. H, T. A. Hecht, and P. M. Roth, 1973: Existing needs in the observational study of atmospheric chemical reactions. U.S. EPA Rep. EPA-R4-73-031, 143 pp.

Siems, S. T., G. D. Hess, K. Suhre, S. Businger, and R. R. Draxler, 2000: A comparison of observed and simulated trajectories of the ACE-1 Lagrangian experiments. *Aust. Meteor. Mag.,* **49,** 109–120.

Sigg, R., and G. Svensson, 2004: Three-dimensional simulation of the ASTEX Lagrangian-1 field experiment with a regional numerical weather prediction model. *Quart. J. Roy. Meteor. Soc.,* **130,** 707–724.

Sollazzo, M. J., L. M. Russell, D. Percival, S. Osborne, R. Wood, and D. W. Johnson, 2000: Entrainment rates during ACE-2 Lagrangian experiments calculated from aircraft measurements. *Tellus,* **52B,** 335–347.

Suhre, K., and Coauthors, 1998: Physico-chemical modeling of the First Aerosol Characterization Experiment (ACE-1) Lagrangian B 1. A moving column approach. *J. Geophys. Res.,* **103,** 16 433–16 455.

Talbot, R., H. Mao, D. Troop, B. Moore, R. Johnson, and S. Businger, 2006: Smart balloon observations over the North Atlantic: Part I—Mini-O_3 sensor sampling of urban plumes. *J. Geophys. Res.,* in press.

Wang, Q., and Coauthors, 1999a: Characteristics of the marine boundary layers during Lagrangian measurements, 1. General conditions and mean vertical structure. *J. Geophys. Res.,* **104,** 21 751–21 766.

——, and Coauthors, 1999b: Characteristics of the marine boundary layers during two Lagrangian measurement periods, 2. Turbulence structure. *J. Geophys. Res.,* **104,** 21 767–21 784.

Wingenter, O. W., M. K. Kubo, N. J. Blake, T. W. Smith, D. R. Blake, and F. S. Rowland, 1996: Hydrocarbon and halocarbon measurements as photochemical and dynamical indicators of atmospehric hydroxyl, atomic chlorine, and vertical mixing obtained during Lagrangian flights. *J. Geophys. Res.,* **101,** 4331–4340.

Wood, R., and Coauthors, 2000: Boundary layer and aerosol evolution during the 3rd Lagrangian experiment of ACE 2. *Tellus,* **52B,** 401–422.

Zak, B. D., 1981: Lagrangian measurements of sulfur dioxide to sulfate conversion rates. *Atmos. Environ.,* **15,** 2583–2591.

Zhuang, L., and B. J. Huebert, 1996: A Lagrangian analysis of the total ammonia budget during ASTEX/MAGE. *J. Geophys. Res.,* **101,** 4341–4350.